Journal of Water Process Engineering 86 (2026) 109916

Contents lists available at ScienceDirect

Journal of Water Process Engineering

journal homepage: www.elsevier.com/locate/jwpe

Charge measurements for optimised NOM characterisation and removal by coagulation

Daniel Ruth [a,b], Bruce Jefferson [a], Ryan Pereira [c], Graeme Moore [b], Peter Jarvis [a,*]

[a] Cranfield University, College Road, Cranfield, Bedfordshire, MK43 0AL, United Kingdom
[b] Scottish Water, Castle House, 6 Carnegie Ave, Pitreavie Castle, Dunfermline, KY11 8GG, United Kingdom
[c] The Lyell Centre, Heriot Watt University, Edinburgh, EH14 4AS, United Kingdom

ARTICLE INFO

Editor: Tzyy Haur Chong

Keywords:
Charge
coagulation
natural organic matter
zeta potential

ABSTRACT

Climatic changes have altered natural organic matter (NOM) characteristics in raw water, intensifying challenges for operation of water treatment systems, particularly the coagulation process. This study explored the measurement of water charge characteristics, in parallel with a range of water quality parameters over an extensive year-long sampling campaign. Results showed variable charge load (15–197 μEq/L) in the raw water throughout the year, attributed to dynamic humic-organic carbon concentrations (1.1–8.3 mg/L) coinciding with increased average rainfall (2.4 mm/day to 6.1 mm/day). Coagulation tests showed a stronger linear relationship between charge load and coagulant demand than for dissolved organic carbon (DOC) concentration (R^2 = 0.80 vs 0.65). This was because the charge characteristics of the water did not change in a consistent way with the NOM concentration, meaning that bulk indicators of organic matter concentration (DOC and UV_{254}) were not always effective for predicting the appropriate coagulant dose. Post-coagulation zeta potential analysis showed minimised DOC residuals at a zeta potential between −10 and 5 mV, with maximum removal achieved when the average zeta potential approached 0 mV. Analysis of the zeta potential distribution provided a new understanding of ideal operating conditions for coagulation. Median zeta potential of −1.69 mV resulted in a condition where at least 68% of all particles were within a range that was effective for charge neutralisation. The study highlights the importance of refining coagulation control methods to address climate-influenced NOM changes, recommending the adoption of UV_{254} coupled with zeta potential as feed-forward and feedback systems, respectively, to provide optimal DOC removal by coagulation.

1. Introduction

Long-term climate change, characterised by rising temperatures and heightened rainfall intensity, has been instrumental in elevating the concentrations and changing the characteristics of natural organic matter (NOM) in many surface waters [1–3]. This exerts greater pressure on the removal processes used at drinking water treatment works (WTW), increasing the need for enhanced treatment and optimisation [4]. When NOM persists across water treatment processes, reactions with chemicals used as disinfectants can form potentially carcinogenic disinfection by-products (DBPs), requiring NOM removal strategies to be optimised [51].

Coagulation is the primary removal method used for bulk removal of NOM from untreated (raw) water [5]. In upland waters, this is predominantly a charge-driven process, where a positively charged metal salt (often aluminium or ferric based) is dosed to reduce the negative charge carried by NOM, facilitating its aggregation and flocculation [6]. Traditionally, the optimum coagulant dose required for a water source is determined by jar testing, which provides valuable empirical data about the removed and residual NOM at variable coagulant concentrations [7]. This method is still commonly used to set seasonal baselines or interrogate treatment issues [8]. A limitation of jar testing, however, is that it is a time-consuming methodology, taking up to two hours per sample, rendering it impractical for responding to real-time compositional changes in the raw water.

Because NOM is negatively charged in water, the addition of a positively charged coagulant reduces this charge and enables NOM compounds to aggregate and form flocs, which are more easily removed from the water. The coagulant dose required to achieve optimised NOM removal is therefore dependent on the charge exerted by the NOM [9].

* Corresponding author.
E-mail address: p.jarvis@cranfield.ac.uk (P. Jarvis).

https://doi.org/10.1016/j.jwpe.2026.109916
Received 15 August 2025; Received in revised form 25 February 2026; Accepted 15 March 2026
Available online 19 March 2026
2214-7144/© 2026 The Authors. Published by Elsevier Ltd. This is an open access article under the CC BY license (http://creativecommons.org/licenses/by/4.0/).

Currently, the absence of tools to measure charge load online necessitates the deployment of surrogate measurements available at WTWs to provide understanding of coagulant demand and water treatability.

Upland waters contain an elevated proportion of high molecular weight aromatic organic compounds, which tend to have a higher degree of hydrophobicity [10]. This NOM portion is also associated with holding a large proportion of the charged material [11]. Therefore, characterisation methods that measure hydrophobicity and molecular weight have been used to provide linkage with NOM treatability by coagulation. For example, UV_{254} can provide an estimation of NOM concentration in upland waters and has been used to create more reactive coagulant dosing algorithms based on absorbance in raw water [9,12]. However, not all NOM components absorb UV at 254 nm, and measurement of waters containing lower concentrations of aromatic compounds may result in an underestimation of NOM concentrations [52]. Alternative spectroscopic methods improve on this limitation by expanding the spectrum to wave scans between 200 and 800 nm measuring the absorption, excitation, and emission of light in the form of 3D fluorescence excitation emission matrices (EEM) based on fluorescence dissolved organic matter (FDOM). This provides a better understanding of the type and source of NOM, identifying humic-like and amino acid-like structures [13]. When coupled with parallel factor analysis (PARAFAC), success in determining OM concentration and character linked to water treatability has been found [14,53]. Fractionation methods that characterise NOM based on molecular weight (MW) and hydrophobicity have also been used [15]. MW fractionation can be performed using size-exclusion liquid chromatography with organic carbon detection (LC-OCD), which separates organic matter based on the size of molecules. Further identification of fractions is based on standard measurements recorded in literature that associates MW size bands to likely molecular weight types [16,17].

For the aforementioned characterisation approaches there is an underlying assumption that the charge density of a water source is consistent, such that a given measured value of a NOM surrogate (for example, UV absorbance, DOC or hydrophobicity) is associated with a particular coagulant dose. Given the dynamic nature of NOM in the environment this assumption needs to be questioned, and long-term seasonal tracking of charge load and density alongside more routinely measured parameters has not been done before, representing a significant research gap. This research therefore presents the first comprehensive investigation into the seasonal fluctuations of charge characteristics in an upland water source dominated by humic substances, and the consequential impact on water treatability by coagulation. The work tested the hypothesis that changes in NOM charge density invalidates the use of many surrogate measures of NOM that assume a constant relationship between organic matter concentration and charge characteristics. This research will advance the current understanding of water quality measurements and their impact on treatment processes through quantifying the charge load present in a raw water source over a one-year period, providing the most detailed continuous insight into NOM charge characteristics to date, improving the ability to understand and manage natural water sources more effectively.

2. Materials and methods

2.1. Raw water sampling and analysis

Raw water samples were collected from a reservoir-fed WTW (WTW A) in Scotland over 10 two-week periods between December 2021 and December 2022. This allowed for monitoring of temporal and seasonal changes in water quality. During these campaigns, hourly samples were collected using an Aquacell P2-multiform auto sampler (Aquamatic, UK). Online UV_{254} absorbance was used to determine if a significant change in water quality had occurred (>10% difference from the base line). When a change was identified, the samples from the hours around this fluctuation were collected for analysis. If no changes were recorded, the 24 samples were collated into two 12-h composite samples. An additional 20 L of water were collected every day to allow for jar testing. Samples were passed through 0.45 μm, pre-rinsed polyether sulfone (PES) filters prior to all non-charge-related analysis.

Coagulated zeta potential and raw charge load were determined using a Zetasizer nano (Malvern Panalytical, UK). For zeta potential measurements, samples were injected into a polystyrene latex-folded capillary cell, equilibrated to 25 °C, and measured in triplicate. The pH was adjusted to 7.0 for all samples to standardise measurement conditions. Zeta potential standards were run monthly to ensure the instrument was performing as expected, and new Zetasizer cells were used for each batch of samples, typically replaced on a monthly basis. After each measurement, cells were rinsed with 100 mL of Milli-Q water followed by sample water, inspected daily for wear, and checked for air bubbles to prevent interference. All data were manually checked to confirm consistency. The zeta potential data was reproducible, with selected replicated measurements being closely bound to the mean value (Fig. S1, Supporting Information, SI). All samples were collected from the same Scottish freshwater reservoir and exhibited low ionic strength. No additional salts were added to the water. While the ionic composition of the reservoir water was not explicitly measured, the consistency of the source and fixed pH for the sample allowed for reliable relative comparisons of zeta potential between samples. Complementary water quality measurements showed broadly similar chemical conditions across samples.

Polydiallyldimethyl ammonium chloride (PDADMAC) (Sigma-Aldrich, UK) was used to determine the charge load of the water from an adapted method described by Finkbeiner et al. [18]. In brief, the pH of raw water was adjusted to 7.0, followed by incremental additions of a diluted PDADMAC solution (416 mg/L) resulting in added concentrations of between 1.0 and 20.0 mg/L of polymer. The zeta potential at each step was measured, and the concentration of PDADMAC needed to reach 0 mV was determined by linear regression. In other words, where the regression line cut across the y axis at 0 mV was the critical polymer concentration. This was validated by collecting multiple data points on either side of the expected 0 mV crossing point (see Fig. S1 for an example titration curve). Since water samples collected over a 24-h period were often split into multiple aliquots with similar characteristics, this provided replication, and any measurements that appeared erroneous were re-analysed to ensure reliability of the regression approach. The added polymer concentration was converted to a charge load using the known charge density of the polymer, 6.2 mEq/g [54]. Total charge density was calculated by normalising the mEq/L to the DOC of the sample to give μEq per g of DOC. Measurement of charge density using this method can be negatively influenced by poor distribution of the polymer into the sample, temperature, instrument drift and the degree of ionisation of NOM compounds. These potential interferences in the approach were mitigated, respectively, by rapidly mixing the sample directly following polymer addition, carrying out experiments in temperature controlled laboratories, regular calibration of the zetasizer, and undertaking the test under regulated pH conditions.

UV_{254} was analysed using a Biochrom Lightwave 3 UV absorbance spectrophotometer (Biochrom, UK, 1 cm quartz cuvette cell). Fluorescence excitation emission matrices (FEEM) from 200 to 800 nm were measured using an Aqualog UV 800C. FEEM results were corrected using UV scans from the Aqualog system (Horiba Scientific, UK, 1 cm quartz cuvette cell). Peak A – humic-like (ex/em = 237–260/400–500 nm) and peak C – humic-like (ex/em = 300–370/400–500 nm) were measured from the FEEM results. The fluorescence freshness index (FI) was also measured as outlined by Ndiweni et al. [19], to provide an indication of NOM age. The FI considers the ratio of the fluorescence emission at 380 nm and the emission between 420 and 435 nm for excitation at 370 nm, where a higher value represents more freshly produced NOM. FEEMs were spectrally corrected for inner filter effects (IFE), instrument-specific correction factors applied, and Rayleigh–Tyndall and Raman

scatter lines were removed. A PARAFAC model of 164 samples generated two components ($C1_{Ex/Em240/438}$ and $C2_{Ex/Em270/499}$) using Solo 9.0 (Eigenvector Research, Inc.). Non-negativity constraints were applied for the model, which was validated by split-half analysis and Openfluor database comparisons (Text S1 and Fig. S2, SI) [20].

DOC was measured using a UV persulfate oxidation method on a M5310 C TOC analyser, calibrated using Sievers standards at 0.1, 1.0, and 10 mg/L (Sievers, UK). Samples measured outside of this analytical range were diluted with 18.2 M Ohm deionised water and blank corrected. The hydrophobicity fractionation was determined using XAD-7 resins. 200 mL/L of the XAD-7 resin were added to a 40 mL sample of the raw water tube and shaken for 6 min at 200 rpm, then allowed to settle for 5 min. The DOC of the supernatant was measured as the transphilic and hydrophilic fraction, and the HPO fraction was calculated by subtracting this from the total DOC, determining the sorbed organic matter. The analysis of the organic compound molecular weight distribution was carried out using liquid chromatography coupled with organic carbon detection (LC-OCD), following the protocols by Pereira et al. [21]. A Model 9 LC-OCD-OND-UVD was used, which had been normalized using humic and fulvic acid standards from the International Humic Substances Society. Peaks were identified using Labview (2013) software. Analytical blanks were routinely run using carbon-free deionised water.

2.2. Coagulation assessment

Jar tests were conducted using a 6-paddle Flocculator SW1 jar tester (Stuart Scientific, United Kingdom) with 1000 mL cylindrical jars. The procedure initiated with preconditioning the water's pH using 1 M sodium hydroxide. A 3-min rapid mix period at 200 rpm followed, where varying doses of coagulant (2.0 to 8.0 mg/L as Al) were added. Coagulant doses were converted to charge load exerted in accordance with existing literature (Table S1, SI). A 15-min flocculation period at 30 rpm and a settling period of 20 min followed. The resulting supernatants were analysed for UV_{254}, FEEM, DOC, MW fraction composition, and zeta potential.

2.3. Data processing

Python and related packages, including NumPy, SciPy, Pandas, and Matplotlib, were used for all data processing, analysis, and visualisation. Linear regression (R^2) was used to assess the correlations between measurement parameters, with values of $p \leq 0.05$ indicating statistical significance. Seasons were used to identify trends in the data and were defined by The Met Office [22] as; spring (March, April, May), summer (June, July, August), autumn (September, October, November), and winter (December, January, February).

3. Results and discussion

3.1. NOM seasonal variability

Water quality was variable over the duration of the trial, with significant ranges in the regularly measured NOM parameters (Table 1). For example, the DOC ranged from 4.95 mg/L to 11.30 mg/L. Charge parameters were also very different, with the charge load having a low of 15.06 μEq/L and a maximum of 197.55 μEq/L. Much of the change was driven by seasonal influences. For example, there was an increase in concentrations of charge load, DOC, HS, UV_{254}, and PARAFAC components from August through to November (Fig. S3, SI). The average monthly DOC increased by 37%, from 6.6 ± 0.2 mg/L in August to 9.5 ± 0.1 mg/L in September, peaking at 11.3 +/− 0.2 mg/L in November. This coincided with increased rainfall from 1.3 to 3.5 mm/day to 4.6–7.5 mm/day. These findings are consistent with previous research that recorded an increase in DOC concentrations by up to 2 times following rainfall due to additional organic matter derived from microbially degraded peatland being flushed into tributaries [23,24]. A 72% increase in charge load from 58 μEq/L to 124 μEq/L was also recorded during this period. This was because peatland generally contains hydrophobic, humic DOC, which can be highly charged. For example, Mergen et al. [25] reported charge densities up to 17 μEq/g DOC for upland water sources, similar to the maximum values observed in this study (Table 1). Minimum concentrations for all parameters were recorded in spring, aligning with seasonally low rainfall (40 mm/month). These observations are comparable with historical DOC measurements in Scotland (2.1–6.1 mg/L) and are consistent with observations in Canadian waters with similar weather and soil compositions (3.2–13.2 mg/L) [14,26].

Table 1
Summary of raw water quality parameters for the water treatment site investigated in this work.

	Unit	Max Value	Min Value	Average (+/− range)
C1	Score	21.82	9.44	14.12 +/− 3.43
C2	Score	18.72	5.69	8.89 +/− 2.60
FEEM-A	Score	1.41	0.05	0.42 +/− 0.16
FEEM-C	Score	0.64	0.03	0.22 +/− 0.08
UV_{254}	cm^{-1}	0.53	0.20	0.34 +/− 0.09
DOC	mg/L	11.30	4.95	7.52 +/− 2.08
$SUVA_{254}$	mg C/L/m	6.85	3.04	4.55 +/− 0.63
BP	mg/L	2.08	0.15	0.93 +/− 0.42
HS	mg/L	8.32	1.05	4.71 +/− 1.74
BB	mg/L	1.57	0.18	0.81 +/− 0.27
LMWN	mg/L	1.87	0.15	0.69 +/− 0.21
Charge load	μEq/L	197.55	15.06	78.39 +/− 50.33
Charge density	μEq/g DOC	18.81	2.37	9.48 +/− 3.84

Yearly average DOC values were similar to those reported in previous studies for upland water sources in Scotland, which varied between 6.4 and 7.4 mg/L, the latter of which included data from the site investigated in this study [6,27]. However, the range found in this research was notably lower than the comparable studies (ΔDOC = 6.3 vs 19.8 and 34.3 mg/L, respectively). This was likely due to buffering from the reservoir feeding this WTW, reducing the impact of DOC flushes, compared to studies that included river-fed systems which are more susceptible to large DOC fluctuations caused by rain-event flushing from the riparian zone. This is supported by Zhao et al. [28], where maximum river water DOC values were 40% greater than lake samples in similar locations.

Concentrations of DOC (3.2–13.8 mg/L), UV_{254} (0.019–0.88 cm^{-1}) and MW fractions (BP: 0.42–0.8, HS: 3.5–7.7, BB: 0.74–2.1 and LMWN: 0.46–1.3 mg/L) were observed, comparable to other humic-laden water sources seen in Australia, Sweden, Canada, and Iran [29–32]. Previous occasional spot measurement of charge load and charge density values were consistent with those found in similar upland peat catchments in Scotland and England (53–210 μEq/L and 6.2–15.0 μEq/DOC) due to the presence of charged HS [33,34].

At the study site, a proportional increase in the charge load and the DOC was observed for DOC concentrations between 4.9 and 7.1 mg/L; thereafter, a rapid increase in charge load relative to DOC was recorded (Fig. 1), showing a significant increase in the charge density of the organic matter. For example, for DOC concentrations between 9.0 and 10.0 mg/L, the charge load increased from 65 to 126 μEq/L. This doubling of charge in the water from a minor change in DOC would notably impact water treatability. Previous work by Bazri and Mohseni [35] reported a similar charge load difference of 41 μEq/L for two samples of similar DOC (8.2 and 8.9 mg/L) but from different locations (antarctica and southern USA). This was attributed to increased aromaticity and molecular weight of the organic matter (3.2 vs 5.2 L/mg/cm^{-1} and 760 vs 1070 Da, respectively). Here, the difference between the low and high DOC charge density for water from the same catchment was attributed to elevated HS concentrations, posited to be flushed into the reservoir from tributaries through peatland following

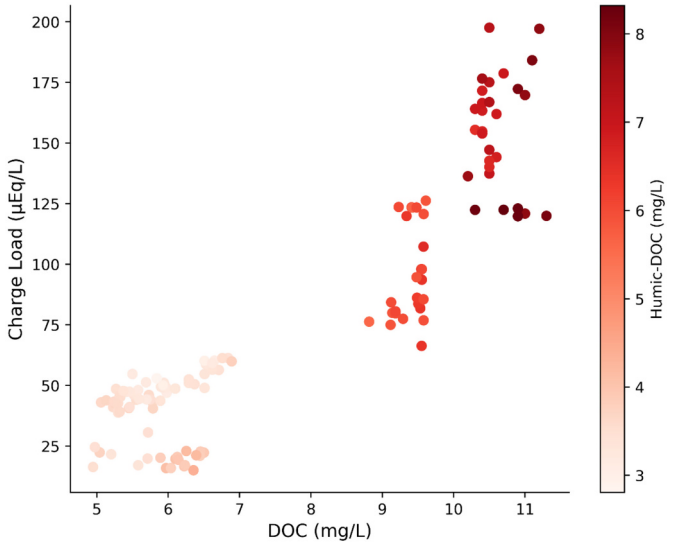

Fig. 1. The charge load of DOC in raw waters sampled at WTW A, showing the concentration of humic-DOC concentrations present in the water.

heavy rainfall. This was supported by the higher freshness index (β: α) values seen in autumn coinciding with these periods of increased rainfall, DOC, and charge load, indicating new NOM was being flushed into the water (Fig. S4, SI). This change in charge density means that the DOC (or surrogate of) will not consistently be an effective proxy for the charge load and hence the coagulant demand. To illustrate, if a nominal fixed coagulant dose ratio of 1 mg Al to 1 mg DOC is applied, with a corresponding charge addition from the coagulant of 12.5 µEq per mg of Al (Table S1, SI), for a water with a DOC of 5.5 mg/L, the equivalence charge balance would be 1.15 $\mu Eq_{Al}/\mu Eq_{DOC}$. When the DOC increases to 10.5 mg/L the dose ratio would be 0.66 $\mu Eq_{Al}/\mu Eq_{DOC}$ due to the increase in charge density of the NOM, representing a significant mismatch in charge addition from the coagulant. Hence the site would be underdosing.

3.2. The impact of charge load on coagulant demand

The disparity between charge load and DOC was further investigated through regular coagulation assessment of the raw water (Fig. 2). Elevated raw water DOC concentrations were recorded in winter (9.4 ± 2.1 mg/L) and autumn (9.4 ± 1.7 mg/L), relative to spring (6.1 ± 0.7 mg/L) and summer (6.6 ± 0.5 mg/L). These DOC increases, however, did not correlate as strongly with the coagulant demand when compared to the charge load ($R^2 = 0.65$ vs 0.80, respectively, Fig. S5, SI). This was because the DOC entering the WTWs between 09/22–12/22 had a higher charge density than that found between 02/22 and 08/22 (13 vs 7 µEq/g DOC), requiring an increased coagulant demand.

To illustrate, to achieve a residual DOC target of 2.0 mg/L required a coagulant dose of 2.0 and 2.5 mgAl/L (25 and 31 µEq/L) in spring. The required dose to achieve the same target DOC residual increased to 3–3.5 mg/L as Al (38–44 µEq/L) in summer. In autumn and winter, a coagulant dose of 8.0 mg/L (100 µEq/L) was required to get near the 2 mg/L DOC residual. This shows a seasonal change in Al: DOC requirement from 0.3 mg Al/mg in spring to 0.5 in summer reaching a maximum of 0.8 in autumn and winter.

The difference in water coagulant demand was further demonstrated when comparing winter samples from 2021 and 2022. Raw water samples collected in December 2021 and November 2022 had similar DOC concentrations (10.1 and 10.6 mg/L, respectively), but the November sample required a 77% increase in coagulant dose to achieve a similar residual DOC concentration. This was because the charge density of the DOC in November was more than double that recorded in December (17 vs 8 µEq/g DOC, respectively) resulting in a notably higher charge load present in the water (169 and 84 µEq/L). This could be explained by an increase in humic-DOC concentrations from 6.0 to 7.5 mg/L, a fraction that has been shown to be highly charged [36] and by an increase in the charge density of the organic matter. These results are consistent with research which found a greater charge load in regenerant from an ion exchange (IEX) process for DOC removal compared to raw water at a similar DOC concentration (51 µEq/L at 13.5 mg/L DOC vs 111 µEq/L at 13.1 mg/L DOC), due to increased concentrations of charged humic substances in the regenerant wastewater [25].

The link between coagulant demand and residual DOC and dose ratio, charge load, and charge density (Al: DOC/CL/CD) were further explored (Fig. 3). In all cases, a decreasing exponential relationship was recorded, where residual DOC was reduced with increasing coagulant-to-NOM ratios, although there was significant variability around a given ratio. The majority of DOC was removed at relatively low ratios for all comparisons. These trends are comparable to those observed by

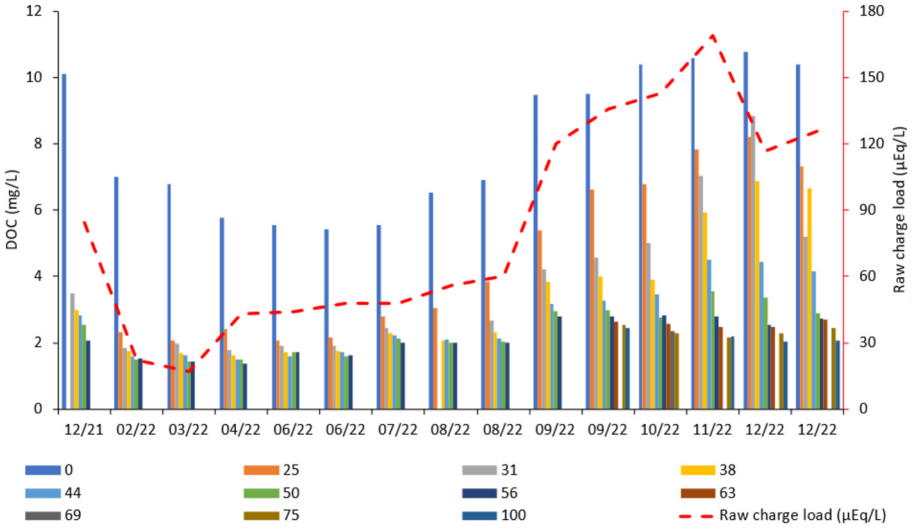

Fig. 2. Residual DOC concentrations following jar tests at coagulant doses displayed as charge exerted from 0 to 0.1 µEq/L (equivalent of 0–8 mg/L as Al). Raw water charge load displayed as a red line on the secondary y-axis. (For interpretation of the references to colour in this figure legend, the reader is referred to the web version of this article.)

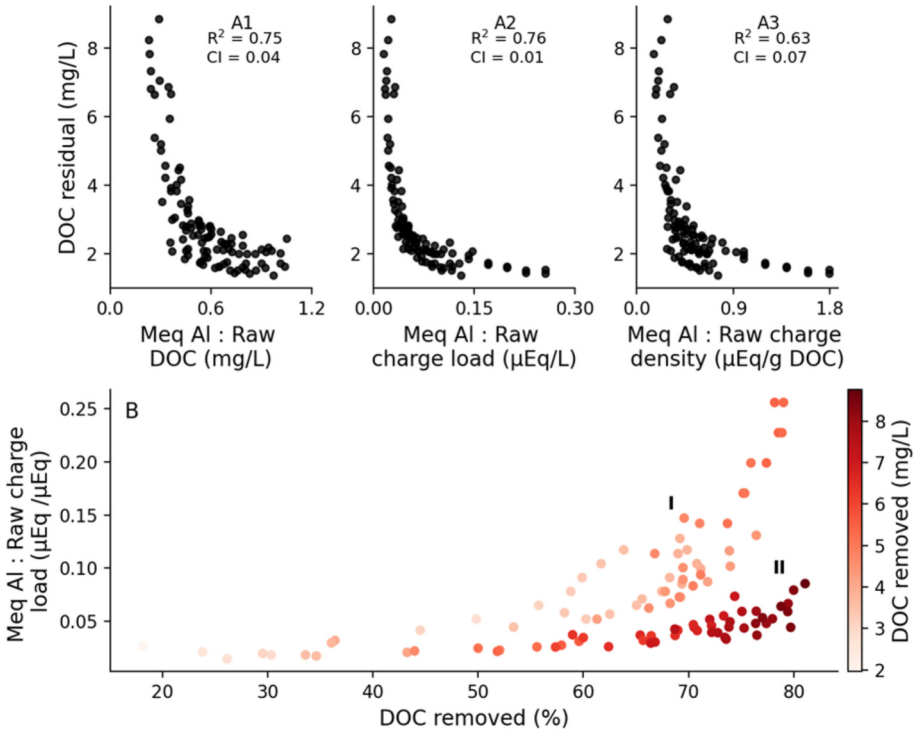

Fig. 3. A) Residual DOC plotted against the coagulant dose ratio with three raw water quality parameters: DOC, charge load and charge density. B) Coagulant to charge load ratio vs DOC % removal, showing two data groups for DOC removal (I: high removal requires high coagulant to charge ratio; and II: high removal requires low coagulant to charge ratio).

Daraei et al. [8], where lower coagulant doses removed the majority of DOC, followed by incremental removal improvements as the dose increased.

The ratio of Al to charge load showed the best fit of the data around the regression curve compared to equivalent data for the water DOC and the charge density, having the lowest confidence interval (CI) ($R^2 = 0.76$ vs 0.75 and 0.63, CI = 0.01 vs 0.04 and 0.07). This shows that the CL had the greatest accuracy in determining the required coagulant dose because ultimately the coagulant demand of the water is dependent on the total charge to be removed.

By ensuring that the correct coagulant dose-to-charge ratio is met, a consistent DOC residual can be achieved, and overdosing can be minimised. This is illustrated by only minor increases in average DOC removal percentages for higher coagulant-to-charge load ratios: 69% for 0.05–0.10, 70% for 0.10–0.15, and 76% for 0.15–0.20. Notably, these increments amount to only a 1% improvement after a 50% increase in coagulant and a 7% increase following a 100% rise in dose.

Analysing the percentage of DOC removed vs the coagulant to CL ratio (Fig. 3B) revealed two different groups of data (I and II) that were classified based on their visual deviation from one another. Group I recorded a higher coagulant:CL demand for DOC removals of over 60% when compared to group II. This was due to lower initial DOC concentrations for group I samples, which overall contained less charged material. This resulted in coagulant:CL ratios of up to 5 times higher for group I samples when compared to those in group II in order to achieve the high DOC removal percentages of >70%. These results are consistent with those found by Sharp et al. [37], where a lower coagulant:DOC dose ratio was required to reach a zeta potential of 0 mV for treatment of waters with a higher initial charge load.

3.3. Zeta potential for coagulation optimisation

The zeta potential following coagulation was further analysed to monitor process optimisation and provide the link between water quality and the neutralisation of charge for effective coagulation

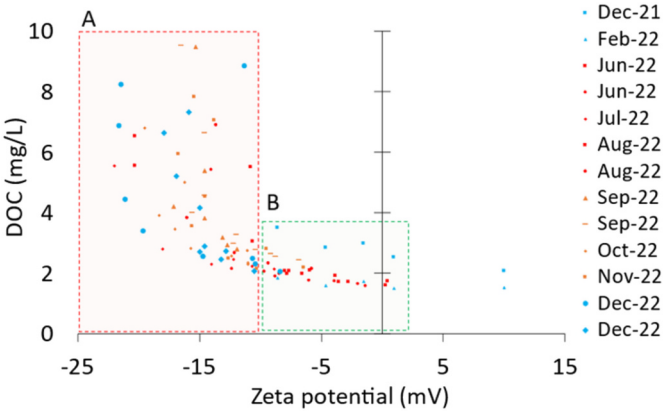

Fig. 4. Residual DOC against coagulated zeta potential. Zone A shows zeta potentials of less than −10 mV showing high and erratic residual DOC, Zone B shows zeta potentials between −10 and + 5 mV showing low and more consistent residual DOC concentrations, with a continued shallow downward trend to 0 mV.

(Fig. 4). This showed optimum DOC removal by coagulation occurring within the zeta potential range of −10 and + 5 mV, following similar trends established by Henderson et al. [34] and Sharp et al. [37].

In this study, two groups of data were identified: group A (< −10 mV), where charge load was not effectively neutralised, resulting in variable DOC removal and frequently high residual organic matter. Similar results were found by Daraei et al. [9] where increased turbidities were recorded when the zeta potential was more negative than −10 mV. These higher residual DOC concentrations may lead to increased DBP concentrations in the final water, causing potential harm to customers and incurring fines where regulatory limits are breached [38,39].

Group B (−10.0 to 2.0 mV) data was synonymous with stable and low DOC residual. The slope of the curve for residual DOC in this group was lower than that for group A. Additionally, a downward trend in DOC residual from 2.7 to 1.8 mg/L was observed as the zeta potential moved towards 0 mV, where complete charge neutralisation occurs. This finding is comparable to work by Hussain et al. [5], where DOC residuals also decreased towards 0 mV. These trends were consistent throughout the year, showing that compositional changes within raw water did not impact on the relationship between residual zeta potential and coagulation optimisation.

Within group B, differences in DOC residual for similar zeta potential values were observed. For example, water from December 2021 saw a DOC residual of 2.5 mg/L at a zeta potential of 1.0 mV, while in February 2022, a similar coagulated zeta potential (0.9 mV) had a lower DOC residual (1.5 mg/L). The composition of the DOC in these samples was analysed and showed an additional 0.5 mg/L of biopolymers, building blocks, and low molecular weight neutrals in the December sample. These organic compounds have been characterised as being hydrophilic in nature and not amenable to coagulation [15]. This was further supported by Sharp [40], who recorded a correlation between initial hydrophilic DOC concentrations and residual DOC ($R^2 = 0.89$) during optimised coagulation.

A further 0.5 mg/L in residual DOC was from an increase in HS. The HS contains the majority of the organic matter charge; however, the "humic" categorization using the LC-OCD is based on a molecular weight cut off at ~1 kDa as well as a UV aromatic response ratio, and may therefore contain non-humic organic compounds [41]. It is therefore feasible that uncharged compounds around ~1 kDa are present within the LC-OCD defined humic fraction. This is a key limitation of rigid categorization of organic compounds which can vary in size and charge. Although valuable information on charged species is provided by this method, further fractional analysis would provide certainty around the specific identification of such organic compounds. Techniques such as Fourier transform ion cyclotron resonance mass spectrometry (FT-ICR-MS) may provide this level of detail as it can determine specific elemental formulae of samples [42,43]. However, this would not provide process optimisation information in real-time.

By considering the UV_{254} of the residual organic matter in both the December 2021 and February 2022 samples, it was possible to estimate the charged species linked with the aromatic compounds present. Low UV_{254} absorbance values were seen in both samples (0.11 and 0.09 cm^{-1}, respectively), suggestive of non-coagulable DOC. These results show that high DOC residuals can be expected when 1) the charge has not been effectively neutralised and 2) non-coagulable NOM is present.

When measuring zeta potential, it is important to acknowledge that the result is the average taken from a distribution of charged particles, with the range varying dependent on the sample characteristics. Previous research on application of zeta potential for water treatment has exclusively focused on the average zeta potential reported, with no analysis of the distribution ([37] and b). It was evident here that for samples that had an average zeta potential of between −10 and + 5 mV, a significant proportion of the distribution was outside could be outside of this range for any given sample. For example, one sample had an average zeta potential of −8.5 mV; however, 61% (912,947/1,496,654 counts) of the particles measured were more negative than −10 mV (Fig. 5). For a sample with an average zeta potential of −2.34 mV, more than 90% of the distribution remained between −10 and + 5 mV. This explained why the DOC residual can increase when operating close to the margins of the optimum range. To further validate this uncertainty in removal at the boundary, a sample with a coagulated average zeta potential at −9.0 mV showed a DOC residual of 3.6 mg/L, while samples within the range of −10.5 to −11.1 mV exhibited DOC residuals of up to 9.0 mg/L.

By analysing the distribution curves of zeta potential measurements ($n = 33$), it was possible to determine a zeta potential condition under which the majority of the distribution remained within the optimised range (Fig. 6). Given that the zeta distribution curves followed an approximate normal distribution, this was considered as the mean ± 1 standard deviation. This was both a statistical and pragmatic approach as it enabled enough data sets to be included in the analysis while ensuring that only those distributions that had a significant majority of their distribution (68%) within the target zeta potential range were included. Using the '68% of the distribution' approach gave an average zeta potential target of −1.7 mV to provide effective DOC removal by coagulation.

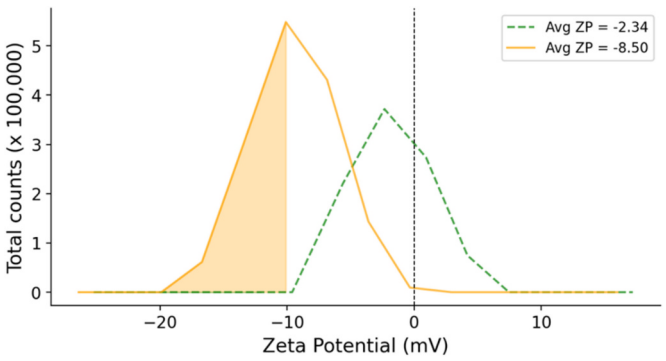

Fig. 5. Zeta potential distribution curve of two surface water samples, both with average values within the optimised zeta potential residual range. The distribution of curve A recorded 61% of all particles below the optimised range, whereas B had all particles within the optimised range.

The zeta potential distributions for real water sources after coagulation are typically broadly spread, with significant tails on either side of the distribution due to differences in the characteristics of the particles and colloids present in any given water source (see Figs. 5 and 6). This meant that for nearly all conditions tested, at least some of the particle distribution was outside of the operational charge window. It would therefore be of significant consequence to be able to undertake further work to explore how the zeta potential distribution can be tightened to ensure that all of the distribution sits within the charge window. Further research is also required to quantify the impact of maintaining the target zeta potential on treated water quality and the universality of this target zeta potential value, considering the variability of different water sources and the influence of seasonal or climatic changes. These factors may alter particle charge characteristics and zeta potential distributions, necessitating a comprehensive understanding of their effects, and nuanced relationships for zeta potential targets at different WTWs.

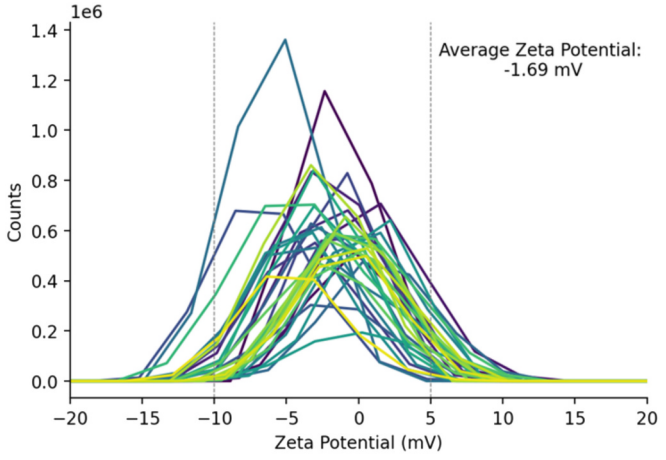

Fig. 6. Zeta potential distribution curves (n = 33) of water samples where 68% of particles have zeta potentials between −10 and 5 mV.

4. Discussion: applying the benefit of charge measurements to operational water treatment systems

An analysis of the linear coefficient of determination of significantly different parameters (R^2, P, 0.05, *t*-test, $n = 137$) was made to assess suitable surrogate measurements for charge load, which is currently only available as a laboratory analysis. By considering the strength of the relationship between water quality parameters and charge load, it was possible to determine which features of NOM aligned most strongly with water treatability (Fig. 7).

Fluorescence analysis revealed weak correlations between charge load and fluorescence peaks A/C ($R^2 = 0.42$ and 0.37, respectively) likely due to their broad wavelength measurement ranges and lack of coverage at 254 nm, a wavelength known to detect humic materials [8]. For example, peak A spans 237–260 nm, therefore, the high absorbance of NOM generally found at UV_{254} may be reduced with the signals from the higher and lower wavelengths. Peak C does not measure UV_{254} at all, as it spans 300–370 nm [55]. PARAFAC analysis provided more specific NOM characterisation, with component 2 more strongly correlating with charge load, but less well than other parameters ($R^2 = 0.66$). Parameters such as $SUVA_{254}$, BP, LMWN, and FEEM peak B, displayed weak ($R^2 < 0.42$) correlations with all water quality parameters. This was due to minimal variation in MW compounds <350 Da and > 20,000 Da and proteinaceous compounds, a common marker for either algal growth [44] or evidence for wastewater discharge in the receiving water [45], neither of which was evident for this reservoir.

Charge load exhibited the strongest correlations with UV_{254}, DOC and HS (Figs. S6–8, SI; $R^2 = 0.72$, 0.86, and 0.79, respectively), consistent with previous research that demonstrated that charge is broadly associated with UV-absorbing aromatic, humic-dominated DOC, common in peatland catchments [33]. All parameters had similar confidence and predictive intervals at a 95% confidence value (LCI = 97–99, UCI = 109–111, LPI = 51–66, UPI = 142–157). The data showed that at lower DOC values (<7.0 mg/L), a stronger correlation was seen, with scatter increasing as the DOC increased (Fig. S7, SI). These results were similar for UV_{254} and humic substances, indicating a more complex composition of the charged species (Fig. S6 and Fig. S8, SI).

While a number of water quality parameters show a reasonable correlation with the charge density, there was still a high degree of scatter when using the best surrogates to determine the optimum coagulant dose for the water. This was shown here to be due to fact that the charge density changes in an inconsistent way with the organic carbon content of the water, a change that can be quite rapid and severe. These changes can be driven by a number of different mechanisms, but largely result from differences in NOM molecular structure and the presence of ionizable functional groups, the degree of dissociation, and the prevailing water quality characteristics (pH and ionic content) [46]. As a result, parameters such as DOC, HS and UV_{254} can never be fully effective when used as a means to model coagulant dose. When charge density was reasonably stable, the coagulant dose demand was a mirror of the change in DOC (or other surrogate). Hence under these conditions, such proxies work effectively to control coagulant conditions. It is during periods of change in charge density that measurement of charge load is required to adequately adjust to the new coagulant demand of the water. This can be achieved through addition of more coagulant dose (to increase the amount of charged metal species being added to the water), as well as a change of coagulation pH (to promote the formation of more charged metal species). These results explain why dosing algorithms for humic rich waters work most of the time, but not always, as they are predicated on surrogates that don't change with the charge density.

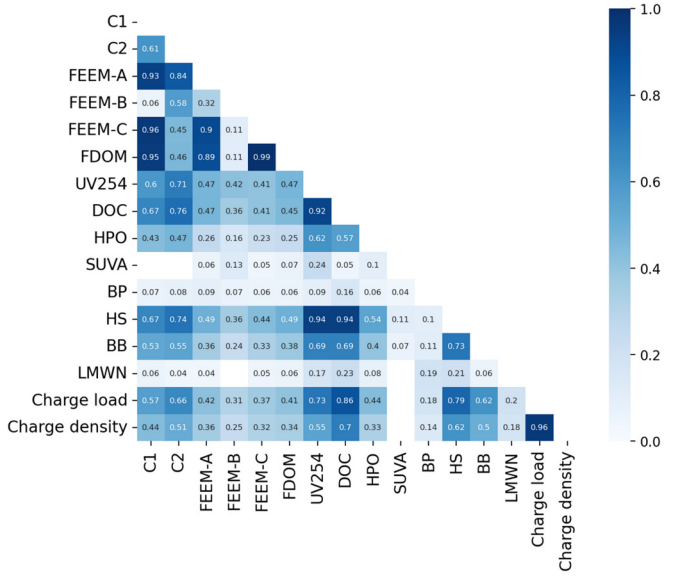

Fig. 7. The coefficient of determination (R^2) of raw water quality parameters measured at the study WTWs between 2021 and 2022, with a colour map indicating the strength of the correlation.

The change in charge density can be detected through regular and routine charge measurement of zeta potential in coagulated water using online or centralised bench-top zeta-meter instruments. For example, the implementation of a coagulation control system that utilises online zeta potential monitoring to adjust coagulant dose automatically with a set point of −1.69 mV would provide fast control and greater confidence in the process for optimised DOC removal. This is an approach that would be particularly valuable for water sources that change character rapidly and often. Some examples of this have been applied in the UK and the US, where municipal WTW adopted online zeta potential to aid in coagulant dosing. Following implementation, both sites reported enhanced clarified turbidity, better downstream efficiency, and reductions in chemical use (by 17–20%) and sludge production (10%) [47,48]. While a full assessment is outside of the scope of this work, the application of online zeta potential instruments at full scale water treatment works needs careful consideration. Regular maintenance is required to ensure the instruments are regularly calibrated (typically, at least monthly), and that the sample delivery system is effectively sustained and free from biofilms and scaling. The benefits of such an approach are likely to make a positive business case at sites where rapid changes in water quality are frequently seen.

For sites that have more stable water quality characteristics, a more cost-effective approach would be to implement routine zeta potential testing in centralised laboratories, serving multiple WTWs. An early signal indicating that the charge density of the organic substances had changed is a more negative or positive residual zeta potential for a fixed coagulant dose to DOC ratio. When this occurs, the charge load should then be measured and the coagulant dose adjusted accordingly to match the change. This procedure can be adopted to both increase and decrease the required coagulant dose.

These approaches would improve upon current post-coagulation monitoring of parameters such as turbidity, which can indicate an issue in treatment process efficiency but does not provide root cause information [49]. This study has shown that small rises in DOC, largely driven by charged HS will notably impact the treatment processes required to remove NOM and that by measuring charge-based parameters in place of current methods, treatment can be improved. The monitoring of charge load, coupled with residual zeta potential post-coagulation, provides possibilities for future enhanced treatment through automation of coagulant control, reducing the impact of climate change on water supply. It is acknowledged that this study only considered a single water source and so more specific data is needed to ensure that relationships hold more universally. However, the approach outlined here could be applied to any source water where charge neutralisation is the driving force behind the coagulation process. More data on charge characteristics are needed across a range of different water

sources in order to understand the variability across multiple water sources with respect to the range and distribution of zeta potential values observed following coagulation.

It is also acknowledged that different types of coagulant (for example ferric versus aluminium based salts) and coagulation pH conditions will change the optimum conditions required. This will largely be driven by the characteristics and charge delivered by the coagulant. For example, it is known that for many water sources, Fe coagulants out-perform Al coagulants with respect to removal of DOC [50]. The operational consequences of these difference being that in order to achieve effective charge neutralisation by coagulation, different ratios of coagulant to DOC in the source water will be required.

The work also highlights that linking catchment management with water treatability needs to extend beyond simpler measures of water quality (such as DOC, UV254 absorbance and colour) and focus on what causes changes in NOM charge density. To the best of the authors' knowledge this has not been done before.

5. Conclusions

Raw water charge measurements have, for the first time, been measured in parallel with common water quality parameters over an extended period of time. This has resulted in the first in-depth dataset that provides a unique view into the seasonal variability of charged species and their impact on the coagulation process.

The water source studied here can be considered representative of an upland reservoir water that contains a reasonably high concentration of DOC and a low level of alkalinity and hardness. However, each water source will have its own unique and dynamic set of characteristics that are influenced by climate, geology, vegetation and anthropogenic activities. In turn, this will influence the conditions required for optimised coagulation of the water. So long as the change in charge characteristics for a given water source can be tracked and responded to, the approach presented here can be applied to any water source where charge neutralisation is the dominant mode of coagulation.

DOC with high charge density significantly increased the coagulant demand of the raw water. This was largely caused when fresh, highly charged, humic-DOC was flushed into water following heavy rainfall in autumn and winter months. This led to the development of a number of important insights on enhanced coagulation control for water sources dominated by NOM. The charge density of the organic matter did not always change with the DOC in a consistent way, meaning that such surrogates can only be used when water quality characteristics are stable. Post coagulation zeta potential provides an effective way of showing when coagulation conditions are optimised, operating around a value −1.69 mV to ensure that the distribution remains largely in a zone that enables effective charge neutralisation. Monitoring the charge load of the water was an effective way of understanding how coagulant dose should be adjusted in order to meet the changing charge demands of the water. The practical consequence of this being that water treatment operators and scientists can have a mechanistic approach to adjusting coagulation conditions to maintain treated water quality, even during periods of significant flux. This is becoming more important as water sources are being impacted by climate change, resulting in more variable water quality.

The key findings of this work are that changes to NOM characteristics (both seasonally and from climate-change impacts) cause changes in charge density of the water that need to be tracked to ensure their optimal removal by coagulation processes. In order to do this, for water sources dominated by DOC, this work recommends the use of UV254 coupled with zeta potential as feed-forward and feedback systems, respectively.

The present research has presented a platform from which coagulation processes can be effectively controlled where charge neutralisation processes dominate. Further work is required to validate the application of the identified target zeta potential to a wider range of water sources. In addition, longer term trials at pilot or full-scale are required in order to be able to confirm the sensitivity and effectiveness of the proposed control strategy.

CRediT authorship contribution statement

Daniel Ruth: Writing – original draft, Methodology, Investigation, Formal analysis, Data curation. **Bruce Jefferson:** Writing – review & editing, Supervision, Conceptualization. **Ryan Pereira:** Writing – review & editing, Supervision, Resources, Methodology. **Graeme Moore:** Writing – review & editing, Resources, Conceptualization. **Peter Jarvis:** Writing – review & editing, Supervision, Funding acquisition, Conceptualization.

Declaration of competing interest

The authors declare that they have no known competing financial interests or personal relationships that could have appeared to influence the work reported in this paper.

Acknowledgements

This research is gratefully supported by the Engineering and Physical Sciences Research Council (EPSRC) through their funding of the WIRe Centre for Doctoral Training (EP/5023666/1) and from the project sponsor Scottish Water. The authors further thank Juliane Bischoff for the laboratory support provided, and Graham Gow for his support at the water treatment works.

Appendix A. Supplementary data

Supplementary data to this article can be found online at https://doi.org/10.1016/j.jwpe.2026.109916.

Data availability

The datasets contributing to this work can be found at https://doi.org/10.57996/cran.ceres-2593.

References

[1] L.E. Anderson, et al., A review of long-term change in surface water natural organic matter concentration in the northern hemisphere and the implications for drinking water treatment, Sci. Total Environ. 858 (2023) 159699. Available at: https://doi.org/10.1016/j.scitotenv.2022.159699.

[2] D.T. Monteith, et al., Dissolved organic carbon trends resulting from changes in atmospheric deposition chemistry, Nature 450 (7169) (2007) 537–540. Available at: https://doi.org/10.1038/nature06316.

[3] C. O'Driscoll, et al., Minimal climate change impacts on natural organic matter forecasted for a potable water supply in Ireland, Sci. Total Environ. 630 (2018) 869–877. Available at: https://doi.org/10.1016/j.scitotenv.2018.02.248.

[4] Ritson, J.P. *et al.* (2014) 'The impact of climate change on the treatability of dissolved organic matter (DOM) in upland water supplies: a UK perspective', Sci. Total Environ., 473–474, pp. 714–730. Available at: doi:https://doi.org/10.1016/j.scitotenv.2013.12.095.

[5] S. Hussain, et al., Coagulation of dissolved organic matter in surface water by novel titanium (III) chloride: Mechanistic surface chemical and spectroscopic characterisation, Sep. Purif. Technol. 213 (2019) 213–223. Available at: https://doi.org/10.1016/j.seppur.2018.12.038.

[6] Golea, D. *et al.* (2017) 'THM and HAA formation from NOM in raw and treated surface waters', Water Res., 112, pp. 226–235. Available at: doi:https://doi.org/10.1016/j.watres.2017.01.051.

[7] A. Sathasivan, et al., Trihalomethane species model for drinking water supply systems, Water Res. 184 (2020) 116189. Available at: https://doi.org/10.1016/j.watres.2020.116189.

[8] Daraei, H., Bertone, E., *et al.* (2023) 'A multi-analytical approach to investigate DOM dynamics and alum dose control in enhanced coagulation process using wide-ranging surface waters', *J. Water Process Eng.*, 56, p. 104368. Available at: doi:https://doi.org/10.1016/j.jwpe.2023.104368.

[9] Daraei, H., Awad, J., *et al.* (2023) 'DOC signal-based alum dose control for drinking water treatment plants', *J. Water Process Eng.*, 54, p. 103934. Available at: doi:https://doi.org/10.1016/j.jwpe.2023.103934.

[10] Jennings, E. *et al.* (2020) 'From highs to lows: changes in dissolved organic carbon in a peatland catchment and lake following extreme flow events', Water, 12(10), p. 2843. Available at: doi:https://doi.org/10.3390/w12102843.

[11] X. Zhu, et al., Prospects for humic acids treatment and recovery in wastewater: A review, Chemosphere 312 (2023) 137193. Available at: https://doi.org/10.1016/j.chemosphere.2022.137193.

[12] Golea, D. *et al.* (2020) 'Influence of granular activated carbon media properties on natural organic matter and disinfection by-product precursor removal from drinking water', Water Res., 174, p. 115613. Available at: doi:https://doi.org/10.1016/j.watres.2020.115613.

[13] Khan, S. *et al.* (2019) 'Fluorescence spectroscopic characterisation of algal organic matter: towards improved: in situ fluorometer development', Environ. Sci. Water Res. Technol., 5(2), pp. 417–432. Available at: doi:https://doi.org/10.1039/c8ew00731d.

[14] Y. Park, et al., Monitoring the influence of wastewater effluent on a small drinking water system using EEM fluorescence spectroscopy coupled with a PARAFAC and PCA statistical approach, Environ Sci Process Impacts 23 (6) (2021) 880–889. Available at: https://doi.org/10.1039/d1em00015b.

[15] K. Brezinski, B. Gorczyca, An overview of the uses of high performance size exclusion chromatography (HPSEC) in the characterization of natural organic matter (NOM) in potable water, and ion-exchange applications, Chemosphere 217 (2019) 122–139. Available at: https://doi.org/10.1016/j.chemosphere.2018.10.028.

[16] N. Her, et al., Optimization of Method for Detecting and Characterizing NOM by HPLC−Size Exclusion Chromatography with UV and On-Line DOC Detection, Environ. Sci. Technol. 36 (5) (2002) 1069–1076. Available at: https://doi.org/10.1021/es015505j.

[17] S.A. Huber, et al., Characterisation of aquatic humic and non-humic matter with size-exclusion chromatography - organic carbon detection - organic nitrogen detection (LC-OCD-OND), Water Res. 45 (2) (2011) 879–885. Available at: https://doi.org/10.1016/j.watres.2010.09.023.

[18] P. Finkbeiner, et al., Understanding the potential for selective natural organic matter removal by ion exchange, Water Res. 146 (2018) 256–263. Available at: https://doi.org/10.1016/j.watres.2018.09.042.

[19] Ndiweni, S.N. *et al.* (2019) 'Assessing the impact of environmental activities on natural organic matter in South Africa and Belgium', Environmental Technology (United Kingdom), 40(13), pp. 1756–1768. Available at: doi:https://doi.org/10.1080/09593330.2019.1575920, Environ. Technol..

[20] K.R. Murphy, et al., OpenFluor– an online spectral library of auto-fluorescence by organic compounds in the environment, Anal. Methods 6 (3) (2014) 658–661. Available at: https://doi.org/10.1039/C3AY41935E.

[21] Pereira, R. *et al.* (2024) 'Investigating the role of hydrological connectivity on the processing of organic carbon in tropical aquatic ecosystems' *Front. Earth Sci.*, 11, p.1250889. Available at: doi:https://doi.org/10.3389/feart.2023.1250889.

[22] The Met Office (2022) *Meteorological spring*. Available at: https://www.metoffice.gov.uk/weather/learn-about/weather/seasons/spring/when-does-spring-start#:~:text=The seasons are defined as,December%2C January%2C February).

[23] D. Anderson, Z. Frogbrook, Sustainable Land Management : Catchment Survey Port Charlotte WTW, Edinburgh, 2016.

[24] L.K. McDonough, D.M. O'Carroll, et al., Changes in groundwater dissolved organic matter character in a coastal sand aquifer due to rainfall recharge, Water Res. 169 (2020), https://doi.org/10.1016/j.watres.2019.115201.

[25] M.R.D. Mergen, et al., Characterisation of natural organic matter (NOM) removed by magnetic ion exchange resin (MIEX® Resin), Water Supply 9 (2) (2009) 199–205. Available at: https://doi.org/10.2166/ws.2009.301.

[26] C. Smeaton, W.E.N. Austin, Distribution of particulate and dissolved organic carbon in surface waters of northern scottish fjords, Estuar. Coast. Shelf Sci. 274 (2022) 107952. Available at: https://doi.org/10.1016/j.ecss.2022.107952.

[27] A. Ferretto, et al., Climate change and drinking water from Scottish peatlands: Where increasing DOC is an issue? J. Environ. Manag. 300 (2021) 113688. Available at: https://doi.org/10.1016/j.jenvman.2021.113688.

[28] Y.Y. Zhao, et al., Formation of N-nitrosamines from eleven disinfection treatments of seven different surface waters, Environ. Sci. Technol. 42 (13) (2008) 4857–4862, https://doi.org/10.1021/es7031423.

[29] F. Chen, S. Peldszus, Ahmed M. Elhadidy, et al., Kinetics of natural organic matter (NOM) removal during drinking water biofiltration using different NOM characterization approaches, Water Res. 104 (2016) 361–370. Available at: https://doi.org/10.1016/j.watres.2016.08.028.

[30] E.E. Lavonen, et al., Tracking changes in the optical properties and molecular composition of dissolved organic matter during drinking water production, Water Res. 85 (2015) 286–294. Available at: https://doi.org/10.1016/j.watres.2015.08.024.

[31] Setareh, P. *et al.* (2020) 'Coupling effect of ozone/ultrasound with coagulation for improving NOM and turbidity removal from surface water', *J. Water Process Eng.*, 37(May), p. 101340. Available at: doi:https://doi.org/10.1016/j.jwpe.2020.101340.

[32] Y. Shutova, et al., Characterisation of dissolved organic matter to optimise powdered activated carbon and clarification removal efficiency, Environ. Sci. Water Res. Technol. 6 (8) (2020) 2065–2077, https://doi.org/10.1039/d0ew00149j.

[33] Finkbeiner, P. *et al.* (2020) 'The combined influence of hydrophobicity, charge and molecular weight on natural organic matter removal by ion exchange and coagulation', *Chemosphere*, 238(124633). Available at: doi:https://doi.org/10.1016/j.chemosphere.2019.124633.

[34] R. Henderson, et al., Identifying the linkage between particle characteristics and understanding coagulation performance, Water Sci. Technol. Water Supply 6 (1) (2006) 31–38. Available at: https://doi.org/10.2166/ws.2006.005.

[35] M. Bazri, M. Mohseni, Impact of natural organic matter properties on the kinetics of suspended ion exchange process, Water Res. 91 (2016) 147–155. Available at: https://doi.org/10.1016/j.watres.2015.12.036.

[36] J. Awad, et al., Modelling of THM formation potential and DOM removal based on drinking water catchment characteristics, Sci. Total Environ. 635 (2018) 761–768. Available at: https://doi.org/10.1016/j.scitotenv.2018.04.149.

[37] E.L. Sharp, et al., Impact of fractional character on the coagulation of NOM, Colloids Surf. A Physicochem. Eng. Asp. 286 (1–3) (2006) 104–111. Available at: https://doi.org/10.1016/j.colsurfa.2006.03.009.

[38] DWQR, Drinking Water Quality in Scotland 2019 Public Water Supply, 2019.

[39] S.N. Ndiweni, et al., PARAFAC model as an innovative tool for monitoring natural organic matter removal in water treatment plants, Water Sci. Technol. 81 (8) (2020) 1786–1796. Available at: https://doi.org/10.2166/wst.2020.136.

[40] E. Sharp, Natural Organic Matter Coagulation. https://dspace.lib.cranfield.ac.uk/bitstream/handle/1826/2224/Sharp-2005.pdf?sequence=1&isAllowed=y, 2005.

[41] L.K. McDonough, H. Rutlidge, et al., Characterisation of shallow groundwater dissolved organic matter in aeolian, alluvial and fractured rock aquifers, Geochim. Cosmochim. Acta 273 (2020) 163–176. Available at: https://doi.org/10.1016/j.gca.2020.01.022.

[42] Y. He, et al., Unraveling the characteristics of dissolved organic matter removed by aluminum species based on FT-ICR MS analysis, Water Res. 255 (2024) 121429. Available at: https://doi.org/10.1016/j.watres.2024.121429.

[43] Leins, A. *et al.* (2023) 'Methods to characterize type, relevance, and interactions of organic matter and microorganisms in fluids along the flow path of a geothermal facility', *Biogeosciences* [Preprint]. Available at: doi:doi:https://doi.org/10.5194/bg-2023-159.

[44] X.-X. Wang, et al., Characterization of algal organic matter as precursors for carbonaceous and nitrogenous disinfection byproducts formation: Comparison with natural organic matter, J. Environ. Manag. 282 (2021) 111951. Available at: https://doi.org/10.1016/j.jenvman.2021.111951.

[45] J. Minier-Matar, et al., Detailed organic characterization of process water to evaluate reverse osmosis membrane fouling in industrial wastewater treatment, Desalination 572 (2024) 117128. Available at: https://doi.org/10.1016/j.desal.2023.117128.

[46] P. Kortelainen, Charge density of total organic carbon in Finnish lakes, Environ. Pollut. 77 (2–3) (1992) 107–113. Available at: https://doi.org/10.1016/0269-7491(92)90066-J.

[47] Fullbright, B., Krumrine, H. and Watson, K. (2014) 'How good is on-line zetapotential measurement in water treatment?', *Water/Waste Processing*, (August 2014).

[48] R. Smith, L. Montalban, F. Hassard, T. Worley, E. Sharp, P. Liu, P. Jarvis, B. Jefferson, Coagulation control using on-line zeta-potential measurements: Can it save money and improve performance? Institute of Water Journal, Issue 3 (2019) 6–7.

[49] M. Campinas, et al., Adsorption/coagulation/ceramic microfiltration for treating challenging waters for drinking water production, Membranes 11 (2) (2021) 1–19, https://doi.org/10.3390/membranes11020091.

[50] P. Jarvis, E. Sharp, M. Pidou, R. Molinder, S.A. Parsons, B. Jefferson, Comparison of coagulation performance and floc properties using a novel zirconium coagulant against traditional ferric and alum coagulants, Water Res. 46 (13) (2005) 4179–4187, https://doi.org/10.1016/j.watres.2012.04.043.

[51] P.D. Nguyen, T.D.Q. Le, N.H. Nguyen, K.T. Tran, M.T. Nguyen, K.A. Huynh, Reducing disinfection byproduct precursors and chlorine consuming substances by a special integration of biofiltration and ozonation: a pilot study, J. Water Process Eng. 37 (2020) 101419.

[52] R. Pereira, C. Isabella Bovolo, R.G.M. Spencer, P.J. Hernes, E. Tipping, A. Vieth-Hillebrand, N. Pedentchouk, N.A. Chappell, G. Parkin, T. Wagner, Mobilization of optically invisible dissolved organic matter in response to rainstorm events in a tropical forest headwater river, Geophys. Res. Lett. 41 (4) (2014) 1202–1208, https://doi.org/10.1002/2013GL058658.

[53] T. Maqbool, J. Zhang, Y. Qin, Q.V. Ly, M.B. Asif, X. Zhang, Z. Zhang, Seasonal occurrence of N-nitrosamines and their association with dissolved organic matter in full-scale drinking water systems: Determination by LC-MS and EEM-PARAFAC, Water Res. 183 (2020) 116096, https://doi.org/10.1016/j.watres.2020.116096.

[54] X. Liu, H. Yin, J. Zhao, Z. Guo, Z. Liu, Y. Sang, Investigation of molecular weight effect on lignin flocculation induced by poly(diallyldimethylammonium chloride) (PDADMAC) through population balance modeling, Sep. Purif. Technol. 254 (2021) 117569, https://doi.org/10.1016/j.seppur.2020.117569.

[55] S. Szerzyna, M. Mołczan, M. Wolska, W. Adamski, J. Wiśniewski, Absorbance based water quality indicators as parameters for treatment process control with respect to organic substance removal, in: E3S Web Conference, Volume 17, 9th Conference on Interdisciplinary Problems in Environmental Protection and Engineering, 2017, https://doi.org/10.1051/e3sconf/20171700091.

https://dspace.org/

Charge measurements for optimised NOM characterisation and removal by coagulation

Ruth, Daniel; Jefferson, Bruce; Pereira, Ryan; Moore, Graeme; Jarvis, Peter

2026-04
Elsevier
https://doi.org/10.1016/j.jwpe.2026.109916
Ruth D, Jefferson B, Pereira R, et al., (2026) Charge measurements for optimised NOM characterisation and removal by coagulation. Journal of Water Process Engineering, Volume 86, April 2026, Article number 109916

Downloaded from a DSpace repository. https://dspace.org/